Aust. J. Phys., 1996, **49**, 335–46

Angular and Polarisation Correlations between Cascade Photons*

J. B. Wang and J. F. Williams

Centre for Atomic, Molecular and Surface Physics, Physics Department,
University of Western Australia, Perth, WA 6009, Australia.

Abstract

The density matrix theory is applied to establish a connection between the configuration of the excited atomic states and the intensity and polarisation of the cascade photons emitted during the decay process. Explicit expressions are obtained for the P, D and F states of hydrogen and helium atoms. These formulae can be used to assist experimental design for the most efficient and revealing measurements. In addition, formulae for the integrated polarisation of the emitted photons from the P, D, F and G states of hydrogen and helium are presented in terms of partial excitation cross sections.

1. Introduction

It is well known that the radiation field emitted by an excited atom is, in general, polarised and anisotropic. By measuring the polarisation and angular distribution of the emitted photons, one can retrieve information on the configuration of the excited atomic states characterised by a wavefunction or a density matrix. Consequently, an understanding of the associated excitation process can be obtained. In fact, the detection of a single line radiation emitted from an atomic state with angular momentum $L = 1$ can provide a complete account for the configuration of this state; while for atoms with angular momentum $L \geq 2$, an analysis of not only the first emitted photon but also the subsequent cascading photon(s) is required for such a complete description.

As an illustration, we plot in Fig. 1 the charge angular distribution of the ^{1}P, ^{1}D and ^{1}F states of helium together with the intensity distribution of the photons emitted directly from these states. The configurations of these states are arbitrarily chosen to be

$$(1)\ \psi_{\mathrm{P}} = 2\varphi_{10} + \mathrm{e}^{\mathrm{i}2\pi/5}(\varphi_{11} - \varphi_{1-1})\,,$$

$$(2)\ \psi_{\mathrm{D}} = \varphi_{20} + 0\cdot 9\mathrm{e}^{\mathrm{i}\pi/2}(\varphi_{21} - \varphi_{2-1}) + 0\cdot 4\mathrm{e}^{\mathrm{i}\pi/3}(\varphi_{22} + \varphi_{2-2})\,,$$

$$(3)\ \psi_{\mathrm{F}} = 0\cdot 4\varphi_{30} + 0\cdot 1\mathrm{e}^{\mathrm{i}\pi/3}(\varphi_{31} - \varphi_{3-1}) + 0\cdot 4\mathrm{e}^{\mathrm{i}\pi/2}(\varphi_{32} + \varphi_{3-2}) + 0\cdot 1\mathrm{e}^{\mathrm{i}\pi/6}(\varphi_{33} - \varphi_{3-3})\,.$$

* Refereed paper based on a contribution to the Advanced Workshop on Atomic and Molecular Physics, held at the Australian National University, Canberra, in February 1995.

0004-9506/96/020335$05.00

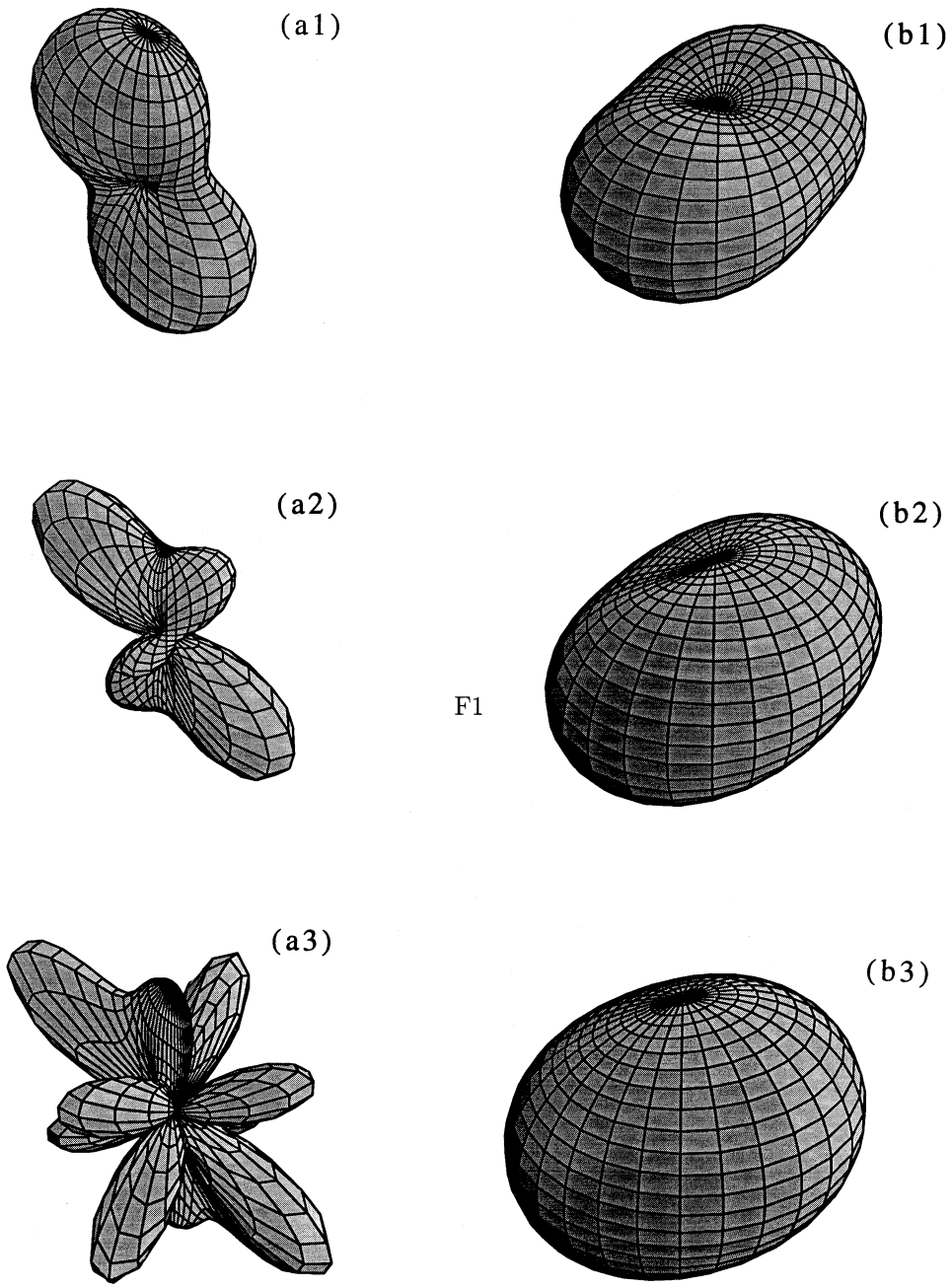

Fig. 1. Left: Angular charge density distribution for the ^{1}P, ^{1}D and ^{1}F states of helium. Right: The intensity distribution of the photons emitted from these states. The configurations of these states are defined in the text.

As shown in Fig. 1, the radiation field of a ^{1}P state has a structure similar to its charge density distribution. As a result, the latter can be determined by measuring the former, and vice versa. However, the radiation field of a ^{1}D state does not possess the complex features of the corresponding charge cloud, rather it is similar to that emitted by a ^{1}P state atom. A measurement of such a simple radiation pattern can only provide partial information on the more complicated charge cloud and hence partial information on the configuration of the atomic state. The same applies to a ^{1}F state, which has an even more complicated charge distribution, while the emitted photon angular distribution is again of a simple form.

On the other hand, excited ^{1}D and ^{1}F states decay to the ground state by several sequential cascade emissions. The cascade photon(s) provide the additional information needed for a complete determination of these atomic states. For example, let us have a closer look at the decay process of the helium 3^1D state. After the excitation, the atom evolves with time until the first photon γ_1 is emitted when the atom decays to the lower 2^1P state. This 2^1P state is in general polarised and the polarisation will be passed on to the second photon γ_2 which is emitted when the atom decays to its ground state. As discussed earlier, a measurement of γ_2 provides complete information on the polarised 2^1P state. This information plus the intensity and polarisation of γ_1 provide sufficient information for a complete determination of the 3^1D state, if γ_1 is measured in coincidence with γ_2 to ensure they come from the same event.

In this paper, we present a general theoretical model for describing the angular and polarisation correlations of the cascading photons. These correlation functions relate the measurable photon intensities and polarisations to the excitation amplitudes of the atom. Explicit expressions for the double and/or triple coincidence measurements of the P, D and F states of atomic hydrogen and helium will be derived. In particular, the integrated polarisation formulae for these states are presented in terms of partial excitation cross sections. In this work, we consider electron-impact excitation, but the theoretical model and the formulae are applicable to any other type of excitation process. In the following model, a pure *LS* coupling scheme is assumed for the helium atom. Wang *et al.* (1995) recently presented a more general treatment for cases with singlet–triplet mixing.

2. Theory

In the case of coherent excitation, the excited atom is in a pure state and thus can be represented by its wavefunction

$$\psi = \sum_m f_m \varphi_m ,$$

which is a linear superposition of its magnetic substates and where f_m are the excitation amplitudes. If the excited atom is in a mixed state, for example when the incident electron beam is unpolarised in spin, a density matrix

$$\rho = \sum_{m'm} f_{m'} f_m^* |\varphi_{m'}\rangle \langle\varphi_m|$$

is required to represent such an atom. One can also use the state-multipole description which is defined as some combination of the density matrix elements, i.e.

$$\langle T(L;t=0)^{\dagger}_{KQ}\rangle = \sum_{m'm}(-1)^{L-m'}\hat{K}\begin{pmatrix} L & L & K \\ m' & -m & -Q \end{pmatrix} f_{m'}f^{*}_{m}$$

with $0 \le K \le 2L$ and $-K \le Q \le K$. The notation $\hat{K} = \sqrt{2K+1}$ is used.

The density matrix formulism and the state multipoles are two equivalent descriptions of an atomic system. However, the state multipoles have the inherent symmetry of the excited atom and hence are usually the preferred representation to use in describing the emitted radiation. For example, the monopole is isotropic and represents the total cross section of the excited state and hence the total intensity of the emitted photons; the rank 1 multipoles represent the orientation of the atom and are related to the circular polarisation of the emitted photons, and the rank 2 multipoles represent the alignment of the atom and are related to the linear polarisation of the emitted photons.

The emitted photons can be fully characterised by a photon density matrix $\rho_{\lambda'\lambda}(\bar{n})$, where λ and $\bar{n} \equiv (\theta, \varphi)$ denote the helicity and Euler angles of the emitted photons. The diagonal elements of this matrix describe the amplitudes of the left and right circular polarisation and so the total intensity $I = \rho_{-1-1}+\rho_{11}$ and the net circular polarisation $P_{3(\mathrm{cir})} = (\rho_{-1-1}-\rho_{11})/I$. The off-diagonal elements describe the phase relationship between the left and right circular polarisation and are associated with the linear polarisations at two perpendicular directions, i.e. $P_{1(\mathrm{lin})} = -(\rho_{-11}+\rho_{1-1})/I$ and $P_{2(\mathrm{lin})} = i(\rho_{-11}-\rho_{1-1})/I$.

Our task is to establish a relationship between the photon density matrix and the state multipoles of the excited atom. In this way, if we know the atomic configurations, we have detailed information on the emitted photons, and vice versa if we measure the intensity and polarisation of the photons we can completely characterise the excited atomic state. Three basic equations are required for such a task (Blum 1981). The first describes the time evolution of the excited atom under its system Hamiltonian H, i.e.

$$\langle T(L;\,t)^{\dagger}_{KQ}\rangle = \langle T(L;\,t=0)^{\dagger}_{KQ}\rangle \,\mathrm{Tr}\{U(t)\,T(L)_{KQ}\,U(t)^{\dagger}\,T(L)^{\dagger}_{KQ}\}\,, \qquad (1)$$

where the time perturbation factor is $U(t) = \mathrm{e}^{-\mathrm{i}Ht/\hbar}$. From the above equation, we have the configuration of the excited state at the time of emitting a photon. The second equation provides the density matrix for the emitted photon

$$\rho_{\lambda'\lambda}(\bar{n}) = C(\omega)\sum_{KQ}\langle T(L;\,t)^{\dagger}_{KQ}\rangle \,\mathrm{Tr}\{r_{-\lambda'}T(L)_{KQ}\,r^{\dagger}_{-\lambda}\}^{\bar{n}}\,, \qquad (2)$$

where $r_{-\lambda}$ is the radiation dipole operator. The third equation gives the configuration of the resultant lower state of the atom,

$$\langle T(L_f;\,t)^{\dagger}_{kq}\rangle^{\bar{n}}_{\lambda'\lambda} = C(\omega)\sum_{kq}\langle T(L;\,t)^{\dagger}_{KQ}\rangle \mathrm{Tr}\{r_{-\lambda'}\,T(L)_{KQ}\,r^{\dagger}_{-\lambda}\,T(L_f)^{\dagger}_{kq}\}^{\bar{n}}\,. \qquad (3)$$

3. Case Study

(3a) Helium 3^1D *State*

Let us apply these three basic equations (1)–(3) to the 3^1D state of helium. At time t_0, the atom is excited to the 3^1D state represented by the state multipoles $\langle T(L_2;\, t=0)^\dagger_{K_2Q_2}\rangle$. This state evolves with time governed by equation (1),

$$\langle T(L_2;\, t)^\dagger_{K_2Q_2}\rangle = \langle T(L_2;\, t{=}0)^\dagger_{K_2Q_2}\rangle \,\mathrm{Tr}\{U(t)\, T(L_2)_{K_2Q_2}\, U(t)^\dagger\, T(L_2)^\dagger_{K_2Q_2}\}\,. \quad (4)$$

The first photon is emitted at time t_1. According to (2), the photon density matrix is

$$\rho_{\lambda_1'\lambda_1}(\bar{n}_1) = C(\omega_1) \sum_{K_2Q_2} \langle T(L_2;\, t_1)^\dagger_{K_2Q_2}\rangle \mathrm{Tr}\{r_{-\lambda_1'}\, T(L_2)_{K_2Q_2}\, r^\dagger_{-\lambda_1}\}^{\bar{n}_1}\,. \quad (5)$$

After emitting the first photon, the atom decays to the 2^1P state which is given by (3) as

$$\langle T(L_1;\, t_1)^\dagger_{K_1Q_1}\rangle^{\bar{n}_1}_{\lambda_1'\lambda_1} = C(\omega_1) \sum_{K_2Q_2} \langle T(L_2;\, t_1)^\dagger_{K_2Q_2}\rangle \times \mathrm{Tr}\{r_{-\lambda_1'}\, T(L_2)_{K_2Q_2}\, r^\dagger_{-\lambda_1}\, T(L_1)^\dagger_{K_1Q_1}\}^{\bar{n}_1}\,. \quad (6)$$

The 2^1P state evolves further with time, i.e.

$$\langle T(L_1;\, t,\, t_1)^\dagger_{K_1Q_1}\rangle^{\bar{n}_1}_{\lambda_1'\lambda_1} = \langle T(L_1;\, t_1)^\dagger_{K_1Q_1}\rangle^{\bar{n}_1}_{\lambda_1'\lambda_1} \times \mathrm{Tr}\{U(t-t_1)\, T(L_1)_{K_1Q_1}\, U(t-t_1)^\dagger\, T(L_1)^\dagger_{K_1Q_1}\}\,. \quad (7)$$

Finally, the second photon is emitted at time t_2 given by the following density matrix:

$$\rho_{\lambda_2'\lambda_2}(\bar{n}_2) = C(\omega_2) \sum_{K_1Q_1} \langle T(L_1;\, t_2,\, t_1)^\dagger_{K_1Q_1}\rangle^{\bar{n}_1}_{\lambda_1'\lambda_1} \mathrm{Tr}\{r_{-\lambda_2'}\, T(L_1)_{K_1Q_1}\, r^\dagger_{-\lambda_2}\}^{\bar{n}_2}\,, \quad (8)$$

and the atom decays to its monople ground state represented by $\langle T(L_0)^\dagger_{00}\rangle$.

By substituting (4), (6) and (7) into equation (8) and calculating the traces over the appropriate quantum numbers, we obtain a two-photon density matrix in terms of the state multipoles of the 3^1D state,

$$\rho_{\lambda_1'\lambda_1,\lambda_2'\lambda_2}(\bar{n}_1,\bar{n}_2) =$$

$$\left(\frac{e^2\omega_1\omega_2}{2\pi c^3\hbar\hat{S}^2}|\langle L_0||\boldsymbol{r}||L_1\rangle||\langle L_1||\boldsymbol{r}||L_2\rangle|\right)^2 \mathrm{e}^{-\gamma_2(t_2-t_1)-\gamma_1 t_1}\sum_{\substack{abpp'\\K_2Q_2K_1Q_1}}(-1)^{K_1+K_2+a}(\hat{K}_1\hat{b})^2\hat{K}_2$$

$$\times\begin{pmatrix}1 & 1 & K_1\\ -\lambda_2' & \lambda_2 & p\end{pmatrix}\begin{pmatrix}K_2 & b & K_1\\ -p' & \lambda_1-\lambda_1' & a\end{pmatrix}\begin{pmatrix}b & 1 & 1\\ \lambda_1-\lambda_1' & \lambda_1' & -\lambda_1\end{pmatrix}$$

$$\times\begin{bmatrix}K_2 & b & K_1\\ L_2 & 1 & L_1\\ L_2 & 1 & L_1\end{bmatrix}$$

$$\times\langle T(L_2;\,t=0)^{\dagger}_{K_2Q_2}\rangle^{\mathrm{lab}}D(\theta\varphi)^{(K_1)}_{pQ_1}\,D(\alpha\beta)^{(K_2)}_{p'Q_2}\,D(\alpha\beta)^{(K_1)}_{aQ_1}\,, \tag{9}$$

where $K_1, b = 0...2$; $Q_1, p, a = -K_1...K_1$; $K_2 = 0...4$; Q_2, $p' = -K_2...K_2$. Details for such a derivation were presented in Wang *et al.* (1995). In the above equation, the first group of terms contains the dipole matrix elements for the first and second photon emission; the second term describes the exponential decay of the initial and intermediate states; the *n-j* symbols are related to the angular momentum coupling and conservation; and the rotational matrices D are geometric factors where $(\alpha,\ \beta)$ and (θ,φ) are the polar angles of the two photon detectors. Finally, the state multipoles $\langle T(L_2;\,t=0)^{\dagger}_{K_2Q_2}\rangle^{\mathrm{lab}}$ represent the excited atom immediately after excitation, where lab refers to the laboratory frame.

As discussed earlier, the sum of the diagonal elements of the photon density matrix gives the total coincidence intensity,

$$I(\alpha\beta,\,\theta\varphi) = \sum_{\substack{\lambda_2'=\lambda_2=\pm1\\ \lambda_1'=\lambda_1=\pm1}}\rho_{\lambda_1'\lambda_1,\lambda_2'\lambda_2}(\alpha\beta,\theta\varphi) = C\sum_{K_2Q_2}A_{K_2Q_2}(\alpha\beta,\,\theta\varphi)\langle T(L_2)^{+}_{K_2Q_2}\rangle^{\mathrm{lab}}\,. \tag{10}$$

The various Stokes parameters are obtained from different combinations of the elements of the two-photon density matrix. For example, if polarisation analysis is performed only on the first photon, the Stokes parameters are given by

$$IP_1 = -\sum_{\lambda_2'=\lambda_2=\pm1}(\rho(\lambda_1=-1;\lambda_1'=1)+\rho(\lambda_1=1;\lambda_1'=-1))$$

$$= C\sum_{K_2Q_2}A^1_{K_2Q_2}(\alpha\beta,\theta\varphi)\langle T(L_2)^{+}_{K_2Q_2}\rangle^{\mathrm{lab}}\,,$$

$$IP_2 = \mathrm{i}\sum_{\lambda_2'=\lambda_2=\pm1}(\rho(\lambda_1=-1;\lambda_1'=1)-\rho(\lambda_1=1;\lambda_1'=-1))$$

$$= C\sum_{K_2Q_2}A^2_{K_2Q_2}(\alpha\beta,\theta\varphi)\langle T(L_2)^{+}_{K_2Q_2}\rangle^{\mathrm{lab}}\,,$$

$$IP_3 = \sum_{\lambda_2'=\lambda_2=\pm 1} (\rho(\lambda_1 = -1; \lambda_1' = -1) - \rho(\lambda_1 = 1; \lambda_1' = 1))$$

$$= C \sum_{K_2 Q_2} A^3_{K_2 Q_2}(\alpha\beta, \theta\varphi) \langle T(L_2)^+_{K_2 Q_2} \rangle^{\text{lab}} . \qquad (11)$$

Evaluations of (10) and (11) were carried out using an algebra program written in *Mathematica* (Wang and Williams 1993) and we obtained the coefficients $A_{K_2Q_2}$ and $A^i_{K_2Q_2}(i = 1, 2, 3)$ for each state multipole. The values for the state multipoles depend upon the associated excitation dynamics and can be obtained by solving the corresponding Schrödinger equation. We calculated these state multipoles for electron-impact excitation in the distorted-wave Born approximation (DWBA) (Madison 1995).

The above theoretical findings can be utilised to provide guidance for optimum experimental settings of the detectors in order to access the most efficient and revealing measurements. For example, in order to fully understand the collision dynamics in the process of exciting a helium atom to the 3^1D state by electronic impact, triple coincidence measurements are required in which the two cascade photons are measured in coincidence with the incident electron. Unfortunately, it was found that the triple coincidence count rate is in general very low. A trial and error type of approach to find the optimum angular locations for the electron and two photon detectors would take excessive time and is not practical in this case.

On the other hand, theoretical predictions for the optimum positioning of the two photon detectors are readily available from (10). The three plots on the left of Fig. 2 show the triple coincidence intensity $I(\alpha, \theta; \beta = \varphi = 0)$, where the detector for the scattered electron is in the plane defined by the two photon detectors. In this figure, (a1), (a2) and (a3) correspond to scattering angles of 5°, 10° and 20° respectively and incident energy of 80 eV. The three plots on the right show the arrangement of the three detectors which gives rise to a maximum coincidence signal according to the DWBA calculation. The angular locations of the two photon detectors are $\alpha = 70°$, $\theta = 110°$ for an electron scattering angle of 5°; $\alpha = 51°$, $\theta = 129°$ for scattering angle 10°; and $\alpha = 40°$, $\theta = 140°$ for scattering angle 20°. Very recently, we also obtained the excitation amplitudes of the 3^1D state at the same incident energy from a convergent close coupling (CCC) calculation by Fursa and Bray (1995). By using their results, the prediction is that, in order to get the maximum triple coincidence signal, the two photon detectors should be placed at $\alpha = 73°$, $\theta = 107°$ for scattering angle 5°; $\alpha = 62°$, $\theta = 118°$ for scattering angle 10°; and $\alpha = 49°$, $\theta = 131°$ for scattering angle 20°.

Equation (10) can also be used inversely, i.e. by measuring the triple coincidence intensity at several different positions, one can extract the experimental values for the state multipoles. Now let us examine the coefficients $A_{K_2Q_2}$ and $A^i_{K_2Q_2}$ $(i = 1, 2, 3)$ which reveal the contribution of each state multipole to the total intensity I and the Stokes parameters. As an example, the coefficients $A^3_{1,1}$, $A^3_{3,1}$, $A^3_{3,2}$ and $A^3_{3,3}$ are shown in Fig. 3, where the minimum and maximum of these functions are clearly seen. If the photon detectors are placed to where a few of the coefficients are zero or small, we can eliminate certain terms in (10) and (11) and focus on the few with large values of $A_{K_2Q_2}$ or $A^i_{K_2Q_2}$ $(i = 1, 2, 3)$.

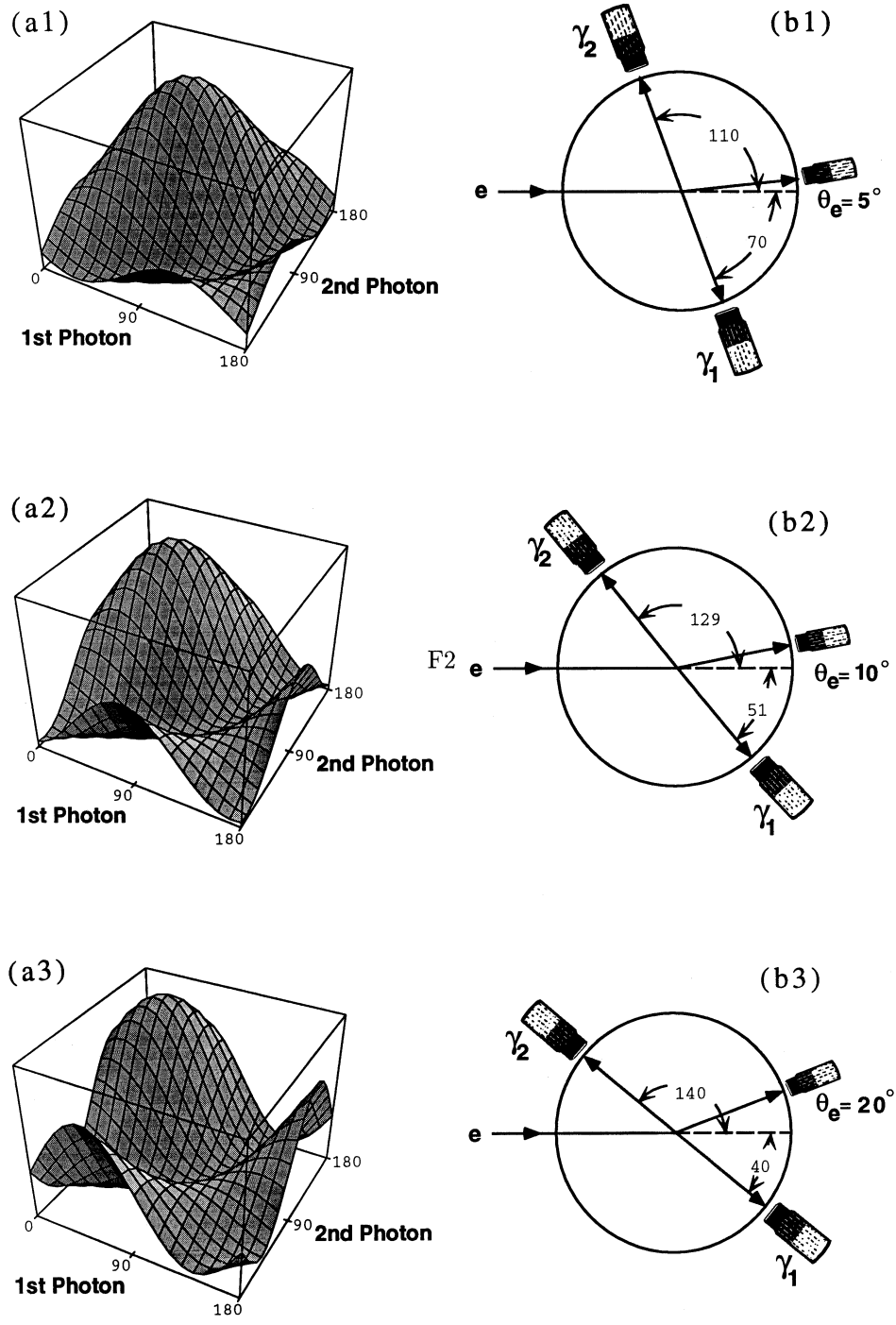

Fig. 2. Left: The triple coincidence intensity distribution $I(\alpha, \theta; \beta = \varphi = 0)$ for electron scattering angles of 5, 10 and 20° and incident energy of 80 eV. Right: The corresponding optimum arrangement of the three detectors.

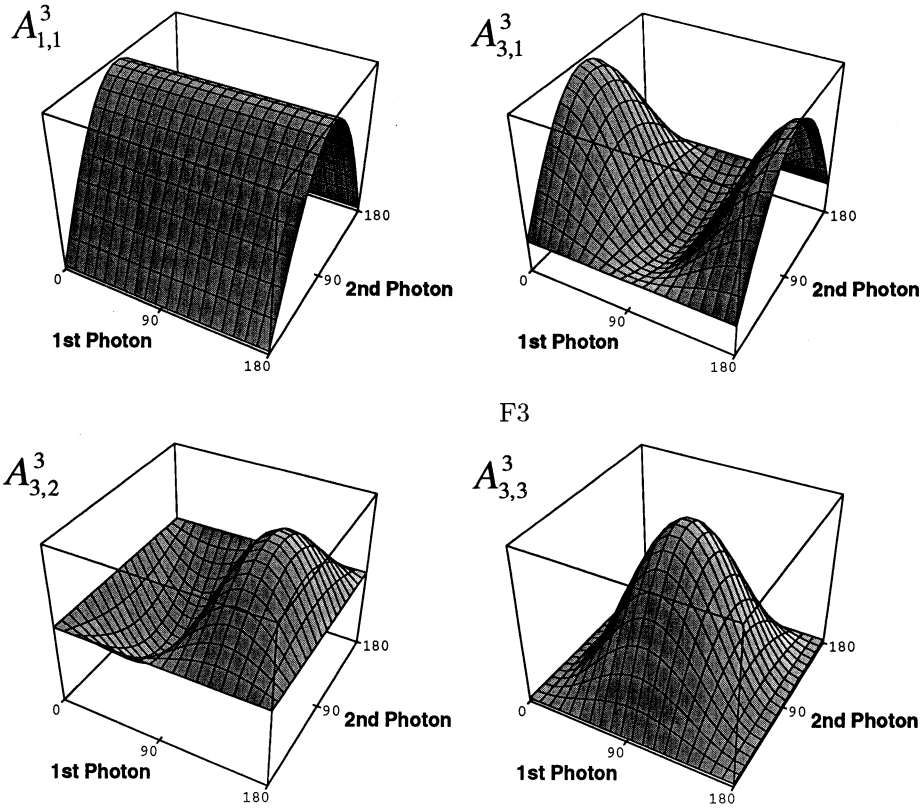

F3

Fig. 3. The coefficients A^3_{KQ} which determine the contribution of each state multipole to the circular polarisation.

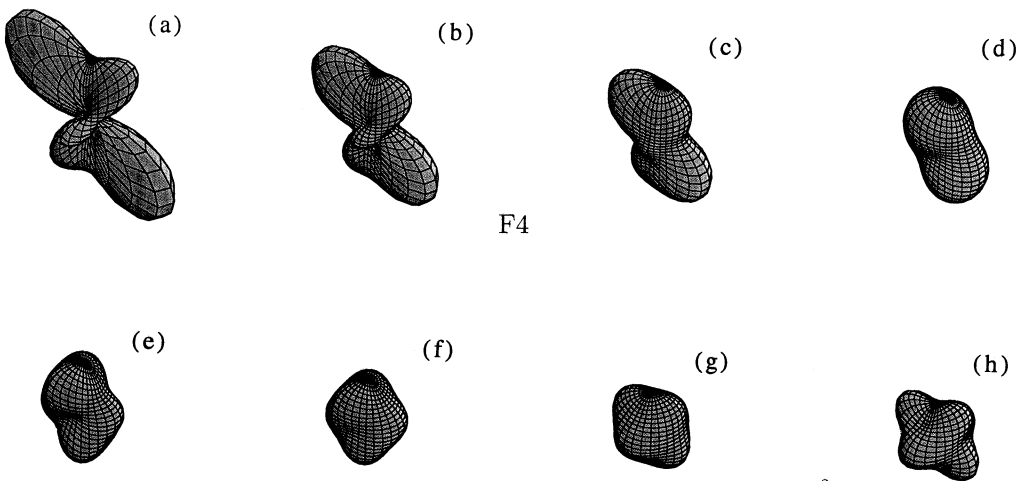

F4

Fig. 4. Time oscillation of the angular charge distribution for the 3^3D state of helium with the same configuration as that shown in Fig. 1(a2). The time sequence a → b → c → d → e → f → g → h → g → f... repeats before the state decays.

(3b) Helium 3^3D State

The main difference between the 3^1D and 3^3D states is that the 3^3D state has a non-zero spin ($S = 1$). During its time evolution, this spin S couples with the angular momentum L resulting in an oscillation of the atomic charge cloud as shown in Fig. 4. Applying the three basic equations (1)–(3) to the decay process of the 3^3D state in the same way as described in the above section, we obtain the two-photon density matrix

$$\rho(t_1\,\lambda_1\,\lambda_1'\,\bar{n}_1,\, t_2\,\lambda_2\,\lambda_2'\,\bar{n}_2)$$

$$= C'(\omega_1\,\omega_2\,t_1\,t_2) \sum_{\substack{K_1 Q_1 K_2 Q_2 a b p p' \\ J_1 J_1' J_2 J_2'}} (-1)^{K+1+J_2+L_2+a+J_1'} (\hat{K}\hat{J}_1\,\hat{J}_1'\,\hat{J}_2\,\hat{J}_2'\,b)^2 \hat{K}_2 \begin{pmatrix} 1 & 1 & K_1 \\ -\lambda_2' & \lambda_2 & p \end{pmatrix}$$

$$\times \begin{Bmatrix} K & L_1 & L_1 \\ L_0 & 1 & 1 \end{Bmatrix} \begin{Bmatrix} L_1 & J_1' & S \\ J_1 & L_1 & K \end{Bmatrix} \begin{Bmatrix} L_2 & J_2' & S \\ J_2 & L_2 & K_2 \end{Bmatrix} \begin{Bmatrix} L_1 & J_1' & S \\ J_2' & L_2 & 1 \end{Bmatrix}$$

$$\times \begin{Bmatrix} L_1 & J_1 & S \\ J_2 & L_2 & 1 \end{Bmatrix} \begin{pmatrix} K_2 & b & K \\ -p' & \lambda_1 - \lambda_1' & a \end{pmatrix} \begin{pmatrix} b & 1 & 1 \\ \lambda_1 - \lambda_1' & \lambda_1' & -\lambda_1 \end{pmatrix} \begin{Bmatrix} K_2 & b & K \\ J_2 & 1 & J_1 \\ J_2' & 1 & J_1' \end{Bmatrix}$$

$$\times \cos(\nu_{J_2' J_2}\, t_1) \cos(\nu_{J_1' J_1}(t_2 - t_1)) \langle T(L_2;\, t_0 = 0)^{+}_{K_2 Q_2} \rangle^{\text{lab}}$$

$$\times D(\theta\varphi)^{(K_1)}_{pQ}\, D(\alpha\beta)^{(K_2)}_{p'Q_2} D^{*}(\alpha\beta)^{(K_1)}_{aQ}\,, \tag{12}$$

where $\nu_{J_2' J_2} = (E_{J_2'} - E_{J_2})/\hbar$ and $\nu_{J_1' J_1} = (E_{J_1'} - E_{J_1})/\hbar$. As expected, this matrix is in a more complicated form in comparison with (11). Also, there are time modulation terms in the above equation, which originate from the spin–orbit interaction and are sometimes called perturbation coefficients. These terms are a direct reflection of the oscillating charge density distribution of the atom shown in Fig. 4.

(3c) Hydrogen 4^2F State

The same approach can also be applied to hydrogen atoms. As an example, we study the 4^2F state of hydrogen, from which three cascade photons are emitted before the state decays to the ground state. We follow the usual steps as described earlier:

- The 4^2F state, represented by the state multipoles $\langle T(L_3)^{\dagger}_{K_3 Q_3} \rangle$, evolves until the first photon is emitted at time t_1 and the atom decays to the 3^2D state

$$\langle T(L_2)^{\dagger}_{K_2 Q_2} \rangle^{\bar{n}_1} = C(\omega_1) \sum_{K_3 Q_3} \langle T(L_3)^{\dagger}_{K_3 Q_3} \rangle G(L_3;\, t)^{K_3}_{J_3 J_3'}$$

$$\times \operatorname{Tr}\{ r_{-\lambda_1}\, T(L_3)_{K_3 Q_3}\, r^{\dagger}_{-\lambda_1'}\, T(L_2)^{\dagger}_{K_2 Q_2} \}^{n_1}\,. \tag{13}$$

- The 3^2D state $\langle T(L_2)^{\dagger}_{K_2Q_2}\rangle^{\bar{n}_1}$ evolves until a second photon is emitted at time t_2 and the atom decays to the 2^2P state

$$\langle T(L_1)^{\dagger}_{K_1Q_1}\rangle^{\bar{n}_2} = C(\omega_2)\sum_{K_2Q_2}\langle T(L_2)^{\dagger}_{K_2Q_2}\rangle^{\bar{n}_1} G(L_2; t-t_1)^{K_2}_{J_2J_2'} \times \mathrm{Tr}\{r_{-\lambda_2'}\, T(L_2)_{K_2Q_2} r^{\dagger}_{-\lambda_2'} T(L_1)^{\dagger}_{K_1Q_1}\}^{\bar{n}_1}. \quad (14)$$

- The 2^2P state $\langle T(L_1)^{\dagger}_{K_1Q_1}\rangle^{\bar{n}_2}$ evolves until a third photon is emitted at time t_3 and then the atom decays to its ground state. The three-photon density matrix is

$$\rho(t_1\lambda_1\lambda_1'\bar{n}_1, t_2\lambda_2\lambda_2'\bar{n}_2, t_3\lambda_3\lambda_3'\bar{n}_3) = C(\omega_3)\sum_{K_1Q_1}\langle T(L_1)^{\dagger}_{K_1Q_1}\rangle^{\bar{n}_2} G(L_1; t_3-t_2)^{K_1}_{J_1J_1'}\,\mathrm{Tr}\{r_{-\lambda_3}\, T(L_1)_{K_1Q_1}\, r^{\dagger}_{-\lambda_3'}\}^{\bar{n}_3}. \quad (15)$$

By substituting (13) and (14) into (15), we have the three-photon density matrix connected with the state multipoles representing the initially excited 4^2F state of hydrogen.

Table 1. Formulae for integrated polarisation in terms of partial cross sections σ_i

Atom	Initial state	Final state	Integrated polarisation
H	^{2}P	^{2}S	$\frac{3(\sigma_0-\sigma_1)}{7\sigma_0+11\sigma_1}$
	^{2}P	^{2}D	$\frac{3(\sigma_0-\sigma_1)}{61\sigma_0+119\sigma_1}$
	^{2}D	^{2}P	$\frac{57(\sigma_0+\sigma_1-2\sigma_2)}{119\sigma_0+219\sigma_1+162\sigma_2}$
	^{2}D	^{2}F	$\frac{57(\sigma_0+\sigma_1-2\sigma_2)}{369\sigma_0+719\sigma_1+662\sigma_2}$
	^{2}F	^{2}D	$\frac{129(2\sigma_0+3\sigma_1-5\sigma_3)}{576\sigma_0+1109\sigma_1+980\sigma_2+765\sigma_3}$
	^{2}F	^{2}G	$\frac{129(2\sigma_0+3\sigma_1-5\sigma_3)}{1262\sigma_0+2481\sigma_1+2352\sigma_2+2137\sigma_3}$
	^{2}G	^{2}F	$\frac{75(10\sigma_0+17\sigma_1+8\sigma_2-7\sigma_3-28\sigma_4)}{1762\sigma_0+3449\sigma_1+3224\sigma_2+2849\sigma_3+2324\sigma_4}$
He	^{1}P	^{1}S	$\frac{\sigma_0-\sigma_1}{\sigma_0+\sigma_1}$
	^{1}P	^{1}D	$\frac{\sigma_0-\sigma_1}{7\sigma_0+13\sigma_1}$
	^{1}D	^{1}P	$\frac{3(\sigma_0+\sigma_1-2\sigma_2)}{5\sigma_0+9\sigma_1+6\sigma_2}$
	^{1}D	^{1}F	$\frac{3(\sigma_0+\sigma_1-2\sigma_2)}{15\sigma_0+29\sigma_1+26\sigma_2}$
	^{1}F	^{1}D	$\frac{3(2\sigma_0+3\sigma_1-5\sigma_3)}{12\sigma_0+23\sigma_1+20\sigma_2+15\sigma_3}$
	^{1}F	^{1}G	$\frac{3(2\sigma_0+3\sigma_1-5\sigma_3)}{26\sigma_0+51\sigma_1+48\sigma_2+43\sigma_3}$
	^{1}G	^{1}F	$\frac{10\sigma_0+17\sigma_1+8\sigma_2-7\sigma_3-28\sigma_4}{22\sigma_0+43\sigma_1+40\sigma_2+35\sigma_3+28\sigma_4}$

(3d) Integrated Polarisations

The explicit expressions of (9), (12) and (15) were obtained with the aid of *Mathematica*. These formulae are rather lengthy and therefore not included in this paper, but they are available from the authors on request. Instead, we present here in Table 1 formulae for the integrated polarisation in terms of the partial cross sections for the G$\Longleftrightarrow$F, F$\Longleftrightarrow$D, D$\Longleftrightarrow$P and P$\Rightarrow$S transitions in hydrogen and helium. These expressions are obtained by integrating (2) over time t and photon angle φ_γ, such as

$$P_1^{\rm int}(\theta_\gamma = 90^\circ) = \int_0^\infty \int_0^{2\pi} IP_1(\theta_\gamma = 90^\circ, \varphi_\gamma)\, {\rm d}\varphi_\gamma\, {\rm d}t \Big/ \int_0^\infty \int_0^{2\pi} I(\theta_\gamma = 90^\circ, \varphi_\gamma)\, {\rm d}\varphi_\gamma\, {\rm d}t\,. \quad (16)$$

A similar integration gives $P_2^{\rm int}(\theta_\gamma = 90^\circ) = P_3^{\rm int}(\theta_\gamma = 90^\circ) = 0$.

In the classic paper of Percival and Seaton (1958), a list of such formulae were given for the lowest few angular momentum states. Recently, Hoekstra *et al.* (1991) presented their results for the F $\rightarrow$ D, D $\rightarrow$ P and P $\rightarrow$ S transitions in hydrogen. However, we found that their formula for the D $\rightarrow$ P transition differs from our result.

4. Conclusion

In this paper, we presented a general theoretical model for describing the angular and polarisation correlations between the cascading photons. These correlation functions relate the measurable photon intensities and polarisations to the excitation amplitudes of the atom. By using the state-multipole description for the excited atom, the photon density matrix of sequential cascade emissions can be derived in an efficient and compact way. These cascade photons, if measured in coincidence, provide complete information about the configuration of the excited atom.

Acknowledgments

This research was supported by the Australian Research Council (ARC) and the University of Western Australia. The authors are indebted to Assoc. Professor A. T. Stelbovics, Professor R. Hippler, Professor D. H. Madison and Dr A. G. Mikosza for many valuable discussions and to Dr I. Bray for sending results prior to publication.

References

Blum, K. (1981). 'Density Matrix Theory and Applications' (Plenum: New York).
Fursa, D. V., and Bray, I. (1995). *Phys. Rev.* A **52**, 1279.
Hoekstra, R., de Heer, F. J., and Morgenstern, R. (1991). *J. Phys.* B **24**, 4025.
Madison, D. H. (1995). Personal communication.
Percival, I. C., and Seaton, M. J. (1958). *Phil. Trans. R. Soc.* A **251**, 113.
Wang, J. B., and Williams, J. F. (1993). *Comput. Phys. Commun.* **75**, 275.
Wang, J. B., Williams, J. F., Stelbovics, A. T., Furst, J. E., and Madison, D. H. (1995). *Phys. Rev.* A, **52**, 2885.

Manuscript received 11 April, accepted 6 June 1996